CHINESE OPTICS LETTERS

Vol. 19, No. 8 | August 2021

Cascaded deep ultraviolet light-emitting diode via tunnel junction

Huabin Yu (余华斌)[1], Zhongjie Ren (任钟杰)[2], Muhammad Hunain Memon[1], Shi Fang (方 师)[1], Danhao Wang (汪丹浩)[1], Zhongling Liu (刘钟灵)[1], Haochen Zhang (张昊宸)[1], Feng Wu (吴 峰)[3], Jiangnan Dai (戴江南)[3], Changqing Chen (陈长清)[3], and Haiding Sun (孙海定)[1*]

[1] School of Microelectronics, University of Science and Technology of China, Hefei 230026, China

[2] Department of Electrical and Computer Engineering, University of California San Diego, La Jolla, CA 92037, USA

[3] Wuhan National Laboratory for Optoelectronics, Huazhong University of Science and Technology, Wuhan 430074, China

*Corresponding author: haiding@ustc.edu.cn

Received December 17, 2020 | Accepted February 2, 2021 | Posted Online April 22, 2021

The AlGaN-based deep ultraviolet (DUV) light-emitting diode (LED) is an alternative DUV light source to replace traditional mercury-based lamps. However, the state-of-the-art DUV LEDs currently exhibit poor wall-plug efficiency and low light output power, which seriously hinder their commercialization. In this work, we design and report a tunnel-junction-cascaded (TJC) DUV LED, which enables multiple radiative recombinations within the active regions. Therefore, the light output power of the TJC-DUV LEDs is more than doubled compared to the conventional DUV LED. Correspondingly, the wall-plug efficiency of the TJC-DUV LED is also significantly boosted by 25% at 60 mA.

Keywords: deep ultraviolet LED; tunnel junction; wall-plug efficiency; AlGaN.

DOI: 10.3788/COL202119.082503

1. Introduction

Deep ultraviolet (DUV) light has various applications in the areas of air/water purification, disinfection, sterilization, and free-space optical communication[1–3]. As an emerging clean DUV light source, AlGaN-based DUV light-emitting diodes (LEDs) have been recognized as a promising candidate to substitute the toxic mercury-based UV lamps. However, the state-of-the-art DUV LEDs still exhibit low light output power (LOP) and poor wall-plug efficiency (WPE)[4]. They are mainly caused by large densities of dislocations/defects[5], the inefficient p-type doping in the Al-rich AlGaN alloys[6], the existence of strong quantum-confined Stark effect[7], and the low light extraction efficiency in the devices[8]. Many efforts have been devoted to addressing the challenges mentioned earlier. Exciting progress has been made to improve the optical performance of the DUV LEDs by either employing novel device structures[9–13] or adopting new growth/epitaxy strategies[14–17].

Recently, the implementation of the tunnel junction (TJ) structure has gained remarkable attention in the development of high-efficiency group-III-nitride-based LEDs. In one aspect, the high-resistance p-type AlGaN contact layer is replaced by a relatively low-resistance AlGaN-based TJ. Therefore, the current injection efficiency can be significantly improved in the DUV LEDs[18,19]. In another aspect, the TJ has been used to construct visible cascaded LEDs[20–24]. Unlike the conventional LED structure with a single active region[25,26], stacked multiple active regions can significantly enhance the optical power due to the repeated electron–hole (e–h) recombination process. So far, such a cascaded structure has not yet been explored in the development of high-efficiency AlGaN-based DUV LEDs. In this work, we tentatively construct a unique DUV LED by cascading two DUV active regions interconnected via a specially designed n^+-AlGaN/p^+-AlGaN TJ. Here, we name it TJ-cascaded (TJC) DUV LED. We found that the output power and WPE of the proposed TJC-DUV LED can be considerably boosted through multiple recombination processes in the cascaded active regions. Then, the underlying physical mechanism of performance enhancement is thoroughly discussed and theoretically analyzed. We believe that the TJC-DUV LED design not only reduces the cost of the fabrication and packaging, but also miniaturizes the LED chip size through vertical integration of two "LEDs" in the pursuit of high-efficiency DUV LEDs of the future.

2. Device Architecture

In this study, three devices are constructed and investigated. Firstly, a conventional DUV LED (C-DUV LED) emitting at 284.5 nm, experimentally reported by Yan *et al.*[27], was utilized

as a reference LED structure. Our physical model and simulation parameters were strictly calibrated to fit our simulated curves with their experimental data to validate our model. As shown in Fig. 1(a), the reference LED structure is composed of a 3-μm-thick n-$Al_{0.6}Ga_{0.4}N$ layer (n-type doping concentration of 5×10^{18} cm^{-3}), five 3-nm-thick $Al_{0.4}Ga_{0.6}N$ quantum wells (QWs) embedded within six 12-nm-thick $Al_{0.5}Ga_{0.5}N$ quantum barriers (QBs), 20-nm-thick p-$Al_{0.65}Ga_{0.35}N$ electron-blocking layer (EBL), 50-nm-thick p-$Al_{0.5}Ga_{0.5}N$ (p-type doping concentration of 1×10^{19} cm^{-3}), and 120-nm-thick p^+-GaN (p-type doping concentration of 1×10^{20} cm^{-3}). Secondly, we also used the same C-DUV LED but with ten QWs in the active region for comparison. Lastly, the TJC-DUV LED consisting of two active regions (each active region has five QWs), which are bridged with a TJ (10-nm-thick p^+-$Al_{0.5}Ga_{0.5}N$/10 nm-thick n^+-$Al_{0.5}Ga_{0.5}N$), is designed, as shown in Fig. 1(b). The n-type and p-type doping concentrations in the TJ are both 1×10^{20} cm^{-3}, according to the reported experimental values[28,29]. It should be noted that the thickness of the n-$Al_{0.6}Ga_{0.4}N$ layer (n-type doping concentration of 5×10^{18} cm^{-3}) for the TJC-DUV LED is thinned to 50 nm for reducing the series resistance of the device. The second active region is built on the 50-nm-thick n-$Al_{0.6}Ga_{0.4}N$ layer with the same parameters, followed by the p-AlGaN layers with the same doping and thickness.

The simulator is provided by Crosslight Inc. APSYS (version 2018), which is widely used in the investigation of the III-nitride-based LEDs in both academia and industry[30]. The Shockley–Read–Hall (SRH) recombination lifetime, the Auger coefficient, and the light extraction efficiency are set as 15 ns, 2.88×10^{-30} cm^6/s, and 13%, respectively. The band offset ratio is set to be 0.5/0.5 for the III-nitride system to fit the power-current (L-I) curves and current-voltage (I-V) curves, which are extracted from the experimental results reported by Yan *et al.*[27]. The polarization-induced charge density is assumed to be 50%, considering the screening effect of defects in the epitaxial layers[31]. Other material parameters used in this work can be found in Ref. [32]. Regarding the tunneling model implemented in this work, we follow the classical model and derivation, which are explained in Ref. [33]. The e–h pair generation rate from band-to-band tunneling in the reverse-biased TJ can be calculated as the following[34]:

$$G(F) = (qFm^*)(2\pi^2h^3)P_0E_{\parallel}, \quad (1)$$

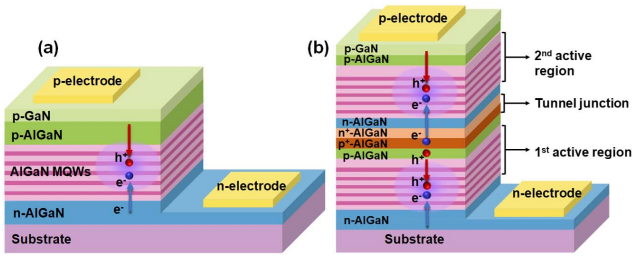

Fig. 1. (a) Schematics of the C-DUV LED and (b) the TJC-DUV LED.

where q is the fundamental electron charge, F is the local field, m^* is the effective tunneling mass, and h is Planck's constant. P_0 is the tunneling probability with a momentum of zero perpendicular. $E_{\parallel}$ is the electron kinetic energy in the tunneling direction. This expression for a local field-dependent generation rate can be subsequently substituted into the drift-diffusion equation solver as a carrier generation term during the III-nitride-based LED operation[14,15].

3. Results and Discussion

The optical performance of the investigated three DUV LEDs is exhibited in Figs. 2(a)–2(d). We found that the simulated results [blue curves in Figs. 2(a) and 2(d)] perfectly matched with those experimental results extracted from the reference LED (orange squares from Yan *et al.*[27]), suggesting the high reliability of the physical parameters and models implemented in this simulation process. As seen in Fig. 2(a), the TJC-DUV LED has an LOP of 14.4 mW at 60 mA, whereas the C-DUV LED devices delivered only 6.7 mW (5 QWs) and 6.2 mW (10 QWs), respectively. In other words, the LOP of the TJC-DUV LED is 114.9% higher than that of the C-DUV LED with five QWs under the same injection current of 60 mA, attributing to a much higher internal quantum efficiency (IQE) of the TJC-LED, which will be discussed later. The great advantages of the TJC-DUV LED can be further confirmed in Fig. 2(b), which shows the electroluminescence (EL) spectra of the C-DUV LED and the TJC-DUV LED. It can be observed that the peak intensity of the TJC-DUV LED shows the highest value, which is consistent with the LOP performance in Fig. 2(a). When introducing a TJC structure, the luminescence intensity is more than doubled, indicating the successful operation of the TJC-DUV LED device.

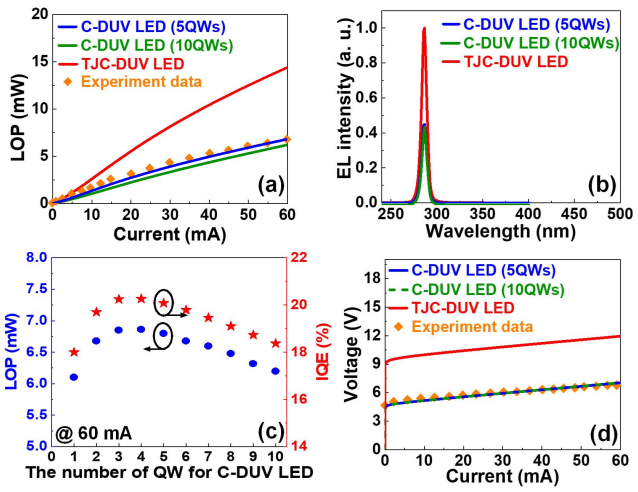

Fig. 2. (a) LOPs as functions of the injection currents for the C-DUV LEDs with five QWs, 10 QWs, and the TJC-DUV LED, respectively. (b) The EL spectra of the three DUV LEDs. (c) The LOPs and IQEs as functions of the number of the QWs in the C-DUV LED at 60 mA. (d) The current-voltage characteristics of the three investigated samples.

There is one question to be answered: can we simply increase the number of QWs to boost the optical performance instead of using a complex TJC structure? In other words, it might not be necessary to build a TJC structure to enhance the performance of the DUV LED device. To address this issue, we investigated the LOP and IQE performance of a C-DUV LED by increasing its number of QWs from 1 to 10. The results are shown in Fig. 2(c). When the QW number increased from 1 to 4, the LOP and IQE of the C-DUV LED can be enhanced dramatically, attributed to the decreased electron current overflow[35]. While if we continuously increase the number of QWs from 5 to 10, the LOP and IQE values decreased abruptly, mainly caused by the limited hole injection efficiency. Therefore, we conclude that it might not be feasible to enhance the optical performance by simply increasing the number of QWs in the C-DUV LED. Instead, the DUV LED performance can be significantly boosted after introducing a TJC structure, as we proposed in this work [Figs. 2(a) and 2(b)]. However, it is certain that the turn-on voltage of the TJC-DUV LED with two interconnected active regions is larger than that of the C-DUV LED with five QWs or 10 QWs [in Fig. 2(d)]. This phenomenon has also been observed in the cascaded visible LEDs previously[13–17] and can be well explained by the doubled built-in electric fields of stacked two active regions in the TJC-LED structures.

The output power of the TJC-DUV LED is much larger than that of the C-DUV LED with the same power supply, as compared in Fig. 3(a). The WPEs for C-DUV LEDs and a TJC-DUV LED are demonstrated in Fig. 3(b). The C-DUV LED with 10 QWs exhibits a lowered WPE than that with five QWs due to the trade-off between the number of QWs and carrier concentration in the active region. In comparison, the WPE of the TJC-DUV LED is significantly increased, resulting from the reduced injection current level at the same value of LOP among the three devices. It can be noted that the WPE of the TJC-DUV LED is a little smaller at a low current level, but it has a much larger value at a high current level than that of the C-DUV LED with five QWs. To be more specific, the WPE of the TJC-DUV LED is significantly boosted by 25% at 60 mA than that of the C-DUV LED with five QWs. It is mainly attributed to the increasing operation bias of the TJC-DUV LED compared with the bias of the C-DUV LED with five QWs.

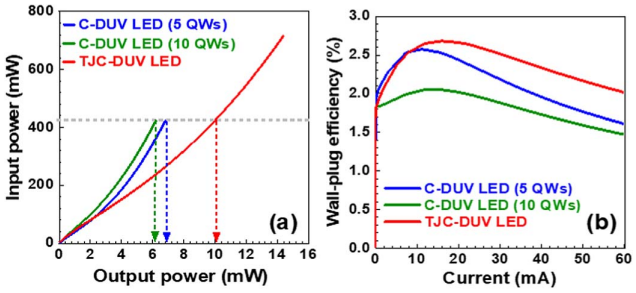

Fig. 3. (a) Required input power of the C-DUV LEDs with five QWs, 10 QWs, and TJC-DUV LED, respectively, as a function of output power. (b) The corresponding WPE values of the three devices as functions of current.

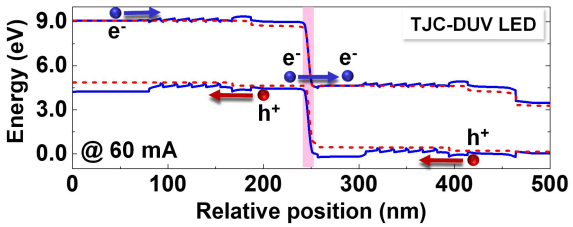

Fig. 4. Energy band diagram for the TJC-DUV LED at 60 mA.

Figure 4 represents the band diagrams of the TJC-DUV LED. In the C-DUV LED, the recombination of the electrons and holes takes place only once within the active region to generate photons. In contrast, the photon generation process can occur in both active regions in the TJC-DUV LED, enabling a dual radiative recombination process, as illustrated in Fig. 4. A mode of smooth carrier transport and injection can be provided by the TJ structure, which bridged the two active regions. Specifically, the electrons in the *p* side move inside the valence band to the TJ, which transfers these valence band electrons into the conduction band of the second active region. In the meantime, the holes in the *p* side of the TJ move in the opposite direction until they reach the first active region. Finally, the photon generation process can be repeated in the second active region of the TJC LED.

The e–h concentrations and radiative recombination rate profiles in the active regions are further investigated to explore the underlying mechanism of the performance enhancement for the TJC-DUV LED. As illustrated in Figs. 5(a1) and 5(b1), the e–h concentration in each QW is drastically reduced when the number of QWs is increased from 5 to 10 in the C-DUV LED. Consequently, the C-DUV LED with 10 QWs exhibits lower

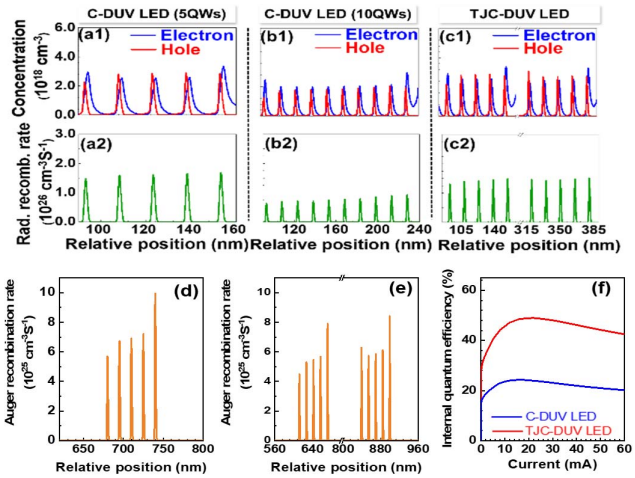

Fig. 5. e–h concentrations within active regions for (a1) the C-DUV LED with five QWs, (b1) the C-DUV LED with 10 QWs, and (c1) the TJC-DUV LED, respectively. The radiative recombination rates within the active regions for (a2) the C-DUV LED with five QWs, (b2) the C-DUV LED with 10 QWs, and (c2) the TJC-DUV LED. The non-radiative recombination rates within the active regions at 60 mA for (d) the C-DUV LED and (e) the TJC-DUV LED. (f) The IQE values of the two devices as functions of current.

radiative recombination rates within the active region in comparison with the C-DUV LED with five QWs, as exhibited in Figs. 5(a2) and 5(b2). On the contrary, the e–h concentration within the two active regions (10 QWs in total) in the TJC-DUV LED remains at the same level as those in the C-DUV LED with five QWs, according to Figs. 5(a1) and 5(c1). The enhanced e–h concentration within the two active regions of the TJC-DUV LED can be ascribed to the dual injection of the electrons and holes in two PIN junctions connected via a TJC structure. Besides, the multiple radiative recombination behavior is also observed in both two active regions, as illustrated in Fig. 5(c2). As shown in Figs. 5(d) and 5(e), the non-radiative recombination rates of the TJC-DUV LED are obviously lower in each QW than that of the C-DUV LED. Hence, with the same radiative rates, the TJC-DUV LEDs possess a significantly higher IQE, as presented in Fig. 5(f), which is attributed to the LOP enhancement of the TJC-DUV LED rather than that of the single C-DUV LED by more than 100%.

4. Conclusion

In summary, we have numerically investigated the unique TJC-DUV LED with cascaded active regions connected by a TJ. The simulation results show that introducing the TJC structure in the DUV LEDs can successfully enable the repeated use of electrons and holes for radiative recombination and consequently produce a significantly enhanced LOP and WPE of the device. The proposed TJC structure provides a reliable and cost-effective method to achieve high-performance DUV LEDs, even possibly in high-power DUV lasers of the future.

Acknowledgement

This work was supported by the National Natural Science Foundation of China (No. 61905236), the University of Science and Technology of China (No. KY2100000081), the Chinese Academy of Sciences (No. KJ2100230003), the Fundamental Research Funds for the Central Universities (No. WK2100230020), and the USTC Research Funds of the Double First-Class Initiative (No. YD3480002002). This work was partially carried out at the USTC Center for Micro and Nanoscale Research and Fabrication. The authors thank the Information Science Center of USTC for hardware/software services.

References

1. H. Sun, S. Mitra, R. C. Subedi, Y. Zhang, W. Guo, J. Ye, M. K. Shakfa, T. K. Ng, B. S. Ooi, I. S. Roqan, Z. Zhang, J. Dai, C. Chen, and S. Long, "Unambiguously enhanced ultraviolet luminescence of AlGaN wavy quantum well structures grown on large misoriented sapphire substrate," Adv. Funct. Mater. **29**, 1905445 (2019).
2. X. Huang, F. Yang, and J. Song, "Hybrid LD and LED-based underwater optical communication: state-of-the-art, opportunities, challenges, and trends," Chin. Opt. Lett. **17**, 100002 (2019).
3. P. Tian, H. Chen, P. Wang, X. Liu, X. Chen, G. Zhou, S. Zhang, J. Lu, P. Qiu, Z. Qian, X. Zhou, Z. Fang, L. Zheng, R. Liu, and X. Cui, "Absorption and scattering effects of Maalox, chlorophyll, and sea salt on a micro-LED-based underwater wireless optical communication," Chin. Opt. Lett. **17**, 100010 (2019).
4. N. Lobo-Ploch, F. Mehnke, L. Sulmoni, H. K. Cho, M. Guttmann, J. Glaab, K. Hilbrich, T. Wernicke, S. Einfeldt, and M. Kneissl, "Milliwatt power 233 nm AlGaN-based deep UV-LEDs on sapphire substrates," Appl. Phys. Lett. **117**, 111102 (2020).
5. Z. Ma, A. Almalki, X. Yang, X. Wu, X. Xi, J. Li, S. Lin, X. Li, S. Alotaibi, M. A. Huwayz, M. Henini, and L. Zhao, "The influence of point defects on AlGaN-based deep ultraviolet LEDs," J. Alloys Compd. **845**, 156177 (2020).
6. N. H. Tran, B. H. Le, S. Zhao, and Z. Mi, "On the mechanism of highly efficient p-type conduction of Mg-doped ultra-wide-bandgap AlN nanostructures," Appl. Phys. Lett. **110**, 032102 (2017).
7. Y.-K. Kuo, J.-Y. Chang, H.-T. Chang, F.-M. Chen, Y.-H. Shih, and B.-T. Liou, "Polarization effect in AlGaN-based deep-ultraviolet light-emitting diodes," IEEE J. Quantum Electron. **53**, 3300106 (2016).
8. S. Zhang, S. Wang, J. Zhang, H. Long, Y. Gao, J. Dai, and C. Chen, "TE/TM mode full-spatial decomposition of AlGaN-based deep ultraviolet light-emitting diodes," J. Phys. D: Appl. Phys. **53**, 195102 (2020).
9. Z. Ren, H. Yu, Z. Liu, D. Wang, C. Xing, H. Zhang, C. Huang, S. Long, and H. Sun, "Band engineering of III-nitride-based deep-ultraviolet light-emitting diodes: a review," J. Phys. D: Appl. Phys. **53**, 073002 (2019).
10. Y. Zheng, J. Zhang, L. Chang, C. Chu, K. Tian, Q. Zheng, Q. Li, Y. Zhang, W. Bi, and Z.-H. Zhang, "Understanding omni-directional reflectors and nominating more dielectric materials for deep ultraviolet light-emitting diodes with inclined sidewalls," J. Appl. Phys. **128**, 093106 (2020).
11. J. Yun and H. Hirayama, "Investigation of the light-extraction efficiency in 280 nm AlGaN-based light-emitting diodes having a highly transparent p-AlGaN layer," J. Appl. Phys. **121**, 013105 (2017).
12. J. W. Lee, G. Ha, J. Park, H. G. Song, J. Y. Park, J. Lee, Y.-H. Cho, J.-L. Lee, J. K. Kim, and J. K. Kim, "AlGaN deep-ultraviolet light-emitting diodes with localized surface plasmon resonance by a high-density array of 40 nm Al nanoparticles," ACS Appl. Mater. Interfaces **12**, 36339 (2020).
13. T. H. Lee, B. R. Lee, K. R. Son, H. W. Shin, and T. G. Kim, "Highly efficient deep-UV light-emitting diodes using AlN-based deep-UV-transparent glass electrodes," ACS Appl. Mater. Interfaces **9**, 43774 (2017).
14. C. Huang, H. Zhang, and H. Sun, "Ultraviolet optoelectronic devices based on AlGaN-SiC platform: towards monolithic photonics integration system," Nano Energy **77**, 105149 (2020).
15. Y. Nagasawa, R. Sugie, K. Kojima, A. Hirano, M. Ippommatsu, Y. Honda, H. Amano, I. Akasaki, and S. F. Chichibu, "Two-dimensional analysis of the nonuniform quantum yields of multiple quantum wells for AlGaN-based deep-ultraviolet LEDs grown on AlN templates with dense macrosteps using cathodoluminescence spectroscopy," J. Appl. Phys. **126**, 215703 (2019).
16. B. So, C. Cheon, J. Lee, J. Lee, T. Kwak, U. Choi, J. Song, J. Chang, and O. Nam, "Epitaxial growth of deep ultraviolet light emitting diodes with two-step n-AlGaN layer," Thin Solid Films **708**, 138103 (2020).
17. T. Wei, S. M. Islam, U. Jahn, J. Yan, K. Lee, S. Bharadwaj, X. Ji, J. Wang, J. Li, V. Protasenko, H. (Grace) Xing, and D. Jena, "GaN/AlN quantum-disk nanorod 280 nm deep ultraviolet light emitting diodes by molecular beam epitaxy," Opt. Lett. **45**, 121 (2020).
18. A. Pandey, W. Shin, J. Gim, R. Hovden, and Z. Mi, "High-efficiency AlGaN/GaN/AlGaN tunnel junction ultraviolet light-emitting diodes," Photon. Res. **8**, 331 (2020).
19. Y. Zhang, S. Krishnamoorthy, F. Akyol, A. A. Allerman, M. W. Moseley, A. M. Armstrong, and S. Rajan, "Design and demonstration of ultra-wide bandgap AlGaN tunnel junctions," Appl. Phys. Lett. **109**, 121102 (2016).
20. J. Piprek, "Origin of InGaN/GaN light-emitting diode efficiency improvements using tunnel-junction-cascaded active regions," Appl. Phys. Lett. **104**, 051118 (2014).
21. Y.-K. Kuo, Y.-H. Shih, J.-Y. Chang, F.-M. Chen, M.-L. Lee, and J.-K. Sheu, "Theoretical investigation of efficient green tunnel-junction light-emitting diodes," IEEE Electron Device Lett. **38**, 75 (2016).
22. Y.-H. Shih, J.-Y. Chang, Y.-K. Kuo, F.-M. Chen, M.-F. Huang, M.-L. Lee, and J.-K. Sheu, "Design of GaN-based multicolor tunnel-junction light-emitting diodes," IEEE Trans. Electron Devices **65**, 165 (2017).

23. S.-J. Chang, W.-H. Lin, and C.-T. Yu, "GaN-based multi quantum well light-emitting diodes with tunnel-junction-cascaded active regions," IEEE Electron Device Lett. **36**, 366 (2015).
24. C. H. Chen, S.-J. Chang, Y.-K. Su, J. K. Sheu, J. F. Chen, C. H. Kuo, and Y. C. Lin, "Nitride-based cascade near white light-emitting diodes," IEEE Photon. Technol. Lett. **14**, 908 (2002).
25. H. Zhao, G. Liu, J. Zhang, J. D. Poplawsky, V. Dierolf, and N. Tansu, "Approaches for high internal quantum efficiency green InGaN light-emitting diodes with large overlap quantum wells," Opt. Express **19**, A991 (2011).
26. H. Zhao, G. Liu, R. A. Arif, and N. Tansu, "Current injection efficiency induced efficiency-droop in InGaN quantum well light-emitting diodes," Solid-State Electron. **54**, 1119 (2010).
27. J. Yan, J. Wang, Y. Zhang, P. Cong, L. Sun, Y. Tian, C. Zhao, and J. Li, "AlGaN-based deep-ultraviolet light-emitting diodes grown on high-quality AlN template using MOVPE," J. Crystal Growth **414**, 254 (2015).
28. Y. Zhang, S. Krishnamoorthy, F. Akyol, S. Bajaj, A. A. Allerman, M. W. Moseley, A. M. Armstrong, and S. Rajan, "Tunnel-injected sub-260 nm ultraviolet light emitting diodes," Appl. Phys. Lett. **110**, 201102 (2017).
29. C.-C. Shen, Y.-T. Lu, Y.-W. Yeh, C.-Y. Chen, Y.-T. Chen, C.-W. Sher, P.-T. Lee, Y.-H. Shih, T.-C. Lu, T. Wu, C.-H. Chiu, and H.-C. Kuo, "Design and fabrication of the reliable GaN based vertical-cavity surface-emitting laser via tunnel junction," Crystals **9**, 187 (2019).
30. http://www.crosslight.com/ (2020).
31. J.-Y. Chang, B.-T. Liou, M.-F. Huang, Y.-H. Shih, F.-M. Chen, and Y.-K. Kuo, "High-efficiency deep-ultraviolet light-emitting diodes with efficient carrier confinement and high light extraction," IEEE Trans. Electron Devices **66**, 976 (2019).
32. H. Yu, Z. Ren, H. Zhang, J. Dai, C. Chen, S. Long, and H. Sun, "Advantages of AlGaN-based deep-ultraviolet light-emitting diodes with an Al-composition graded quantum barrier," Opt. Express **27**, A1544 (2019).
33. J. L. Moll, *Physics of Semiconductors* (McGraw-Hill, 1964).
34. M. F. Schubert, "Interband tunnel junctions for wurtzite III-nitride semiconductors based on heterointerface polarization charges," Phys. Rev. B **81**, 035303 (2010).
35. S. Tan, J. Zhang, T. Egawa, and G. Chen, "Influence of quantum-well number and an AlN electron blocking layer on the electroluminescence properties of AlGaN deep ultraviolet light-emitting diodes," Appl. Sci. **8**, 2402 (2018).